# Modeling Study on Non-Uniform Lateral Distribution in Large-Scale Circulating Fluidized Bed Boilers

Boyu Deng[1], Yi Zhang[2], Man Zhang[1], Hairui Yang[1,*], and Guangxi Yue[1]

**DOI:** 10.1002/cite.202200078

***Dedicated to Prof. Dr.-Ing. Joachim Werther on the occasion of his 80th birthday***

With the development of the circulating fluidized bed (CFB) combustion technology, the cross-sectional area of the boiler furnace increases gradually, making the lateral non-uniform distribution in the furnace more prominent. To investigate the flow field inhomogeneity in the furnace, a two-dimensional mass balance model was established in this work, and the lateral solid concentration deviation was adopted to evaluate the degree of the flow field inhomogeneity. Afterwards, the effect of four factors on the lateral non-uniform distribution was examined. It turned out that the lateral profile of the primary air flow rate had a much greater influence than that of the coal feeding rate.

**Keywords:** 2D modeling, Fluidization model, Large-scale CFB boilers, Lateral dispersion, Non-uniform distribution

*Received:* May 25, 2022; *revised:* August 15, 2022; *accepted:* September 19, 2022

## 1 Introduction

Prof. Joachim Werther has made great achievements in the field of gas-solid flow during his academic career and published over two hundred papers up to now. In 1972 he received his doctoral degree from Erlangen University, and in 1976 he completed his habilitation at the same university. Shortly afterwards, he joined BASF AG in Ludwigshafen, where he published his first journal paper in *Chemie Ingenieur Technik*. In 1980 he was appointed Professor at Hamburg University of Technology where he headed the Institute of Solids Process Engineering and Particle Technology until his retirement in 2008.

Looking back Prof. Werther's academic career, it can be found that his research interests include measuring techniques for multiphase (mainly gas-solid) flow systems [1–8], fluidized bed combustion characteristics of sewage sludge and coal [9–17], particle attrition in fluidized-bed systems [18–27], gas and solid mixing behavior in fluidized-bed reactors [28–37], modeling of industrial/large-scale fluidized-bed reactors [38–44], flowsheet simulation of solids processes [45–51], and more recently, chemical looping processes [52–58]. From all his research work, it can be seen that Prof. Werther always pays attention to the scaling effect (non-uniform/maldistribution) in fluidized bed reactors. Early in 1977, he published a paper named *Problems of scaling-up fluidized-beds* to make discussions on this issue [59], and later he continued to dig into this field by carrying out comprehensive research on the gas and solid mixing characteristics in fluidized-bed reactors [28–37]. With the knowledge obtained, Prof. Werther successfully quantified the mixing of the gas and solid phase with the introduction of dispersion coefficients, and established models of industrial/large-scale circulating fluidized bed (CFB) boilers/combustors capable of describing the uneven reactants distribution [38–44], reminding us to focus more on the non-uniform distribution in CFB boilers.

Nowadays, with the further increase of the capacity of CFB boilers, the cross-sectional area of the furnace increases accordingly, resulting in more severe maldistribution in the lateral direction of the furnace, and thus great importance should again be attached to this topic. Considering that the hydrodynamic characteristics such as the solid concentration profile determine the distribution of the combustion fraction, heat flux and temperature and thus have a profound impact on the combustion and heat transfer processes [60, 61]. To develop a deeper understanding of the maldistribution phenomenon in the furnace and maintain the safe, stable and high-efficiency operation of CFB boilers, the lateral non-uniform distribution of flow parameters should be investigated first.

[1]Boyu Deng, Dr. Man Zhang, Prof. Hairui Yang, Prof. Guangxi Yue
yhr@mail.tsinghua.edu.cn
State Key Laboratory of Power Systems, Department of Energy and Power Engineering, Tsinghua University, Beijing 100084, China.
[2]Dr. Yi Zhang
China Electric Power Planning & Engineering Institute, Beijing 100120, China.

  

Commonly speaking, the research methods to study the gas-solid flow behaviour can be divided into two categories: experimenting and modeling. Given the complexity and total cost of carrying out a series of field tests in industrial CFB boilers, the modeling approach was favored in this work. Based on the dynamics of the gas-solid flow, the numerical models of CFB boilers can be distinguished into two kinds: computational fluid dynamics (CFD) model and fluidization model (also known as semi-empirical model) [62]. By solving the mass, momentum, and energy conservation equations for gas and solid phases, CFD models can offer a detailed description of the three-dimensional flow field in CFB boilers. On the contrary, by introducing semi-empirical submodels (derived from abundant experiments or field test data), fluidization models can directly determine some important flow parameters, such as the axial profile of the solid concentration and the solid mass flow rate. Therefore, compared with CFD models, fluidization models are generally more computationally efficient and can also give a high-accuracy prediction of the basic feature of the gas-solid flow in CFB boilers [63], which makes fluidization models well suited for the investigation of the gas-solid flow behavior in industrial CFB boilers. Furthermore, with respect to the dimension of spatial discretization, fluidization models can be classified into zero-dimensional (0D), one-dimensional (1D), core-annular (1.5D) and two-dimensional (2D) [64]. Considering that the focus of this work was on the lateral non-uniform distribution in the CFB furnace, the two-dimensional fluidization model was adopted.

In this work, based on the 1D model developed by Yang [63], an 2D mass balance model of industrial CFB boilers was established to probe the lateral non-uniform distribution of solid particles in the furnace. The field test data obtained in a 300-MW single-furnace CFB boiler were used to determine the key input parameters of the model. Afterwards, by introducing the concept of lateral solid concentration deviation, the effect of the lateral profile of the coal feeding rate, primary air flow rate and cyclone efficiency as well as the value of the lateral dispersion coefficient on the lateral non-uniform distribution was analyzed and compared.

## 2 Model Description

The two-dimensional mass balance model established in this work consists of a furnace and a cyclone. The desulfurization, combustion, and heat transfer process are not taken into account, and it is assumed that the feeding materials are ash particles formed through the drying, pyrolysis, and combustion process. Given that the discrepancy between the prediction results under the above simulated conditions and the actual values is mainly due to the inaccurate description of the temperature distribution in the CFB furnace, the prediction results at full load would be affected only to a limited extent as under the given circumstances a uniform distribution of the furnace temperature can be assumed, and the same value can be used for the temperatures at different heights.

Since only the lateral non-uniform distribution at full load is explored in this work, ignoring the influence of such processes on the solid concentration in the furnace can be justified. Besides, the effects of the ash formation characteristics, solid attrition and particle segregation are all included in the proposed 2D model, and more details can be found in the previous study [63].

To investigate the non-uniform distribution in the lateral direction, the CFB furnace was discretized in both the vertical and lateral direction, with $N$ cells along the vertical direction and $M$ cells (depends on the number of cyclones) along the lateral (width) direction, as demonstrated in Fig. 1. Considering the wide size distribution of bed materials, solid particles were divided into $N_k$ different particle groups according to the diameter and $N_l$ age groups based on the residence time.

For each cell ($i$, $j$), the mass balance of solid particles in size group $k$ and age group $l$ was established (shown in Fig. 2) and incorporated in a FORTRAN program, and is described as follows:

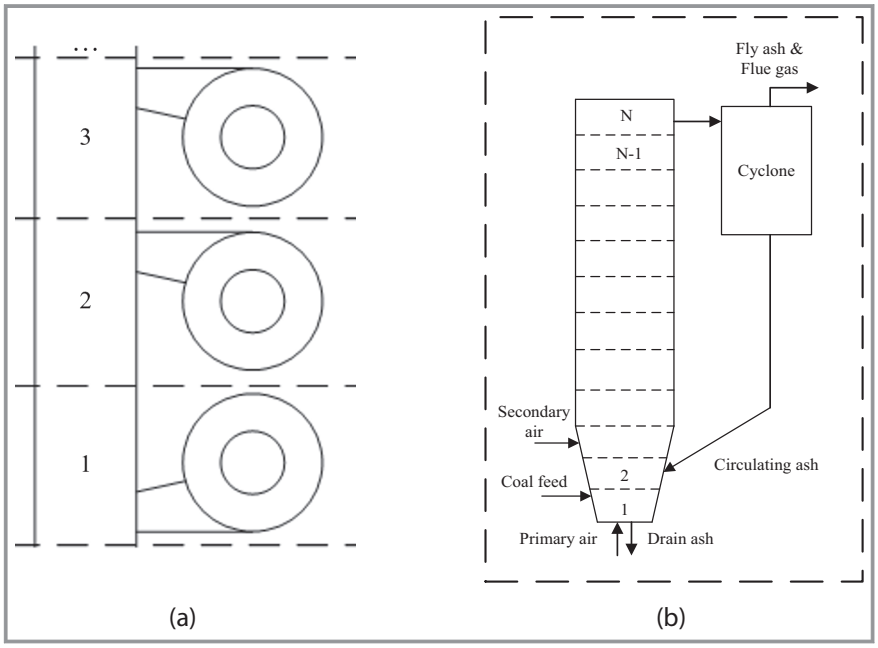


**Figure 1.** Cell structure of the 2D mass balance model. a) Spatial discretization in the lateral direction; b) spatial discretization in the vertical direction.

  

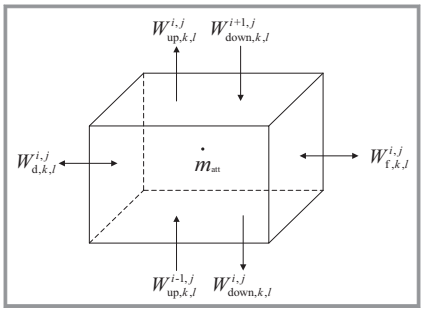


**Figure 2.** Mass balance of solid particles in each cell.

$$W^{i,j}_{fa,k,l} + W^{i,j}_{ra,k,l} - W^{i,j}_{da,k,l} + W^{i-1,j}_{up,k,l} - W^{i,j}_{up,k,l} - W^{i,j}_{down,k,l} + W^{i+1,j}_{down,k,l} + W^{i,j}_{left,k,l} - W^{i,j}_{right,k,l} + \dot{m}_{shift,k,l} + \dot{m}_{l-1\to l} - \dot{m}_{l\to l+1} = 0 \quad (1)$$

where $W$ denotes the solid mass rate, while subscripts *fa, ra, da, up, down, left* and *right* represent feeding ash, recirculating ash, drainage of bottom ash, upwards solid, downwards solid, leftwards solid and rightwards solid. $\dot{m}_{shift,k,l}$ is the solid mass rate caused by particle attrition, and $\dot{m}_{l-1\to l}$ ($\dot{m}_{l\to l+1}$) represent the age decline of solid particles.

According to previous studies [65, 66], although the mechanism of lateral dispersion in the dense bed is different to that in the dilute zone, the values of the lateral dispersion coefficient in these two regions are similar, which varies from 0.001 to 0.01 $m^2s^{-1}$. Therefore, for the sake of convenience, the dispersion coefficients in dense phase and dilute zone ($D_{sr}$ and $D_{gr}$) were set to be identical in this model and were assumed to be in the range of 0.001–0.004 $m^2s^{-1}$, which is well within the range of the measurement and prediction results reported in previous literature [67–72]. In light of this, the solid mass flux between lateral cells can be determined as:

$$W^{i,j}_{L(R),k,l} = D_{sr(gr)} \frac{\partial C^{i,j}_{k,l}}{\partial x} A^i_{sec} \quad (2)$$

where $C$ represent the solid concentration, and $A_{sec}$ is the section area between lateral cells.

## 3 Numerical Setup

A 300-MW subcritical CFB boiler was chosen as the simulation object in this work, which consists a furnace with dimensions 31.9 m × 9.6 m × 47.6 m (height) and three thermal insulated cyclones. Therefore, in the aforementioned model, 3 cells were divided in the lateral direction, and were named as A, B and C, which corresponds to the cell on the left, in the middle and on the right, as illustrated in Fig. 3.

The effect of four influential factors, namely the lateral profile of the coal feeding rate, primary air flow rate and cyclone efficiency as well as the value of the lateral dispersion coefficient, on the lateral non-uniform distribution was investigated in this work, which produced a total of 15 calculation cases. Based on the field test data at full load, the key input parameters for different calculation cases were set and listed in Tab. 1. For the convenience of narration, all the values in the column of the coal feeding rate and primary air flow rate were normalized, and the unit value here stands for 20.50 $kg\,s^{-1}$ and 43.49 $Nm^3s^{-1}$, respectively. Besides, the $d_{99}$ of the three cyclones were all set as 120 µm, while the $d_{50}$ of the cyclone in cell B was varied from 27 to 41 µm to examine the influence of cyclone efficiency.

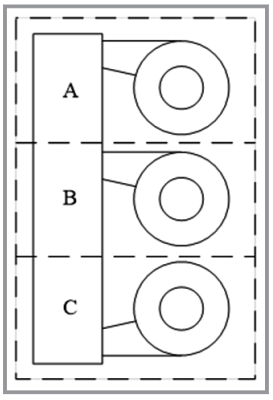


**Figure 3.** Division of cells in the lateral direction.

## 4 Results and Discussion

### 4.1 Calculation Results

With the established 2D mass balance model, the vertical profile of the solid concentration in the furnace as well as the mass flow rate and mass averaged particle size of the fly ash, bottom ash and circulating ash under different calculation cases were predicted, as demonstrated in Fig. 4 and Tab. 2. From Fig. 4a, it turns out that in case 1, the solid concentration in the three cells is almost the same at all axial elevations, proving that solid particles are evenly distributed when the input parameters are identical. However, once the coal feeding rate (case 4), primary air flow rate (case 7) or cyclone efficiency (case 11) deviates from the average value, the inhomogeneous distribution of particles in the lateral direction becomes obvious.

To better compare the prediction results of different calculation cases and quantitatively evaluate the degree of the flow field inhomogeneity in the lateral direction, the mean square error of the solid concentration in the cells at the same axial elevation $\sigma_C(i)$ and the height-averaged mean square error of the solid concentration $\sigma_C$ were adopted as the indicators, as expressed in Eq. (3) and (4).

$$\sigma_C(i) = \sqrt{\left[\sum_j \left(C^j(i) - \overline{C}(i)\right)^2\right]/(M-1)} \quad (3)$$

  

**Table 1.** Key input parameters for different calculation cases. Coal feeding rate and primary air flow rate were normalized, with the unit value 20.50 kg s$^{-1}$ and 43.49 Nm$^3$s$^{-1}$, respectively.

| Case | $D_{sr(gr)}$ [m$^2$s$^{-1}$]a) | Coal feeding rate $W_{fa}$ | | | Primary air flow rate $Q_{pr}$ | | | $d_{50}$ [μm] | | |
|---|---|---|---|---|---|---|---|---|---|---|
| | | A | B | C | A | B | C | A | B | C |
| 1 | 0.001 | 1 | 1 | 1 | 1 | 1 | 1 | 34 | 34 | 34 |
| 2 | 0.001 | 0.95 | 1.1 | 0.95 | 1 | 1 | 1 | 34 | 34 | 34 |
| 3 | | 0.9 | 1.2 | 0.9 | | | | | | |
| 4 | | 0.85 | 1.3 | 0.85 | | | | | | |
| 5 | 0.001 | 1 | 1 | 1 | 0.95 | 1.1 | 0.95 | 34 | 34 | 34 |
| 6 | | | | | 0.9 | 1.2 | 0.9 | | | |
| 7 | | | | | 0.85 | 1.3 | 0.85 | | | |
| 8 | 0.001 | 1 | 1 | 1 | 1 | 1 | 1 | 34 | 41 | 34 |
| 9 | | | | | | | | 34 | 37 | 34 |
| 10 | | | | | | | | 34 | 31 | 34 |
| 11 | | | | | | | | 34 | 27 | 34 |
| 12 | 0.000 | 0.9 | 1.2 | 0.9 | 1 | 1 | 1 | 34 | 34 | 34 |
| 13 | 0.002 | | | | | | | | | |
| 14 | 0.003 | | | | | | | | | |
| 15 | 0.004 | | | | | | | | | |

a) Due to the limitation of the adopted equation solution method, $D_{sr(gr)}$ has to be lower than 0.005 m$^2$s$^{-1}$, otherwise the FORTRAN program will crash. Therefore, in this work, only the cases with $D_{sr(gr)}$ = 0.001–0.004 m$^2$s$^{-1}$ are presented.

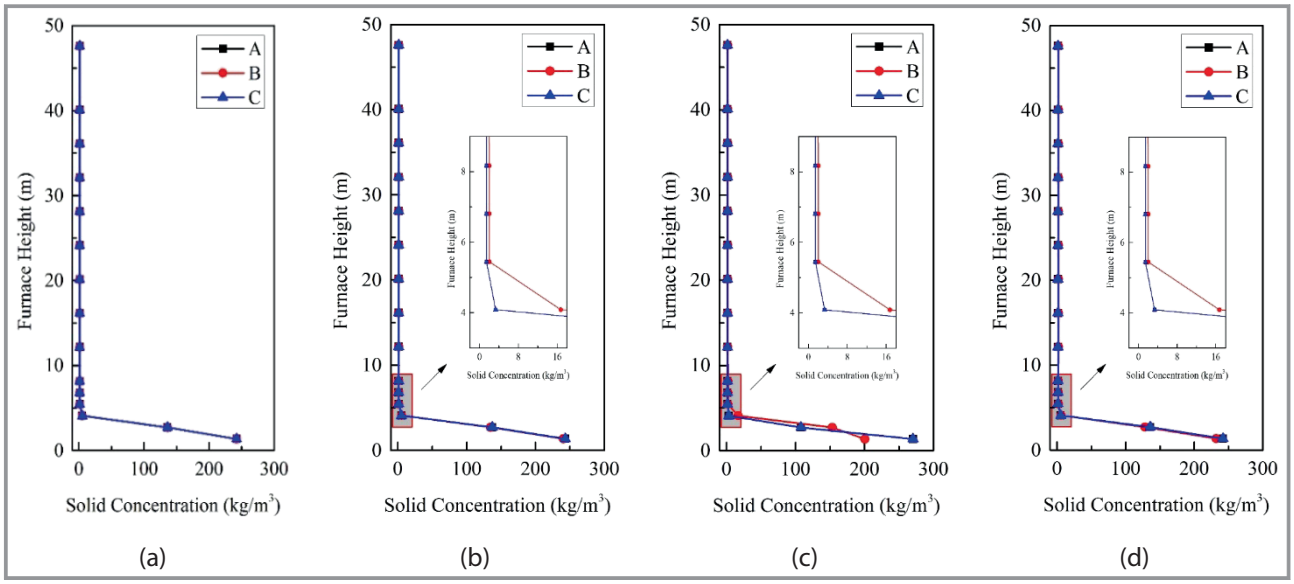


**Figure 4.** Vertical profile of the solid concentration in the furnace under different cases. a) Case 1, b) case 4, c) case 7, d) case 11.

where $C^j(i)$ is the solid concentration in cell ($i$, $j$), while $\overline{C}(i)$ is the cross-sectional averaged solid concentration at the height of cell ($i$, $j$ = 1 – $M$).

$$\sigma_C = \frac{1}{H}\int_0^H \sigma_C(i)\mathrm{d}h_i \tag{4}$$

where $H$ is the height of the furnace, and $h_i$ is the height of cell ($i$, $j$ = 1 – $M$).

**Table 2.** Prediction results for different calculation cases.

| Case | Mass flow rate [kg s$^{-1}$] | | | | | | Mass averaged particle size [μm] | | | | | |
|---|---|---|---|---|---|---|---|---|---|---|---|---|
| | Fly ash | | Bottom ash[a)] | | Circulating ash | | Fly ash | | Bottom ash[a)] | | Circulating ash | |
| | A (C) | B | A (C) | B | A (C) | B | A (C) | B | A (C) | B | A (C) | B |
| 1 | 1.52 | 1.52 | 0.83 | 0.83 | 355.57 | 355.57 | 42.77 | 42.77 | 387.13 | 387.13 | 161.08 | 161.08 |
| 2 | 1.46 | 1.64 | 0.77 | 0.94 | 349.97 | 366.27 | 42.79 | 42.71 | 390.60 | 380.68 | 161.51 | 160.29 |
| 3 | 1.40 | 1.75 | 0.71 | 1.06 | 344.19 | 376.32 | 42.81 | 42.63 | 394.22 | 374.79 | 161.98 | 159.57 |
| 4 | 1.34 | 1.87 | 0.65 | 1.18 | 338.29 | 385.69 | 42.82 | 42.55 | 397.99 | 369.44 | 162.49 | 158.91 |
| 5 | 1.51 | 1.54 | 0.84 | 0.80 | 350.85 | 364.63 | 42.87 | 42.54 | 379.15 | 402.83 | 160.72 | 162.01 |
| 6 | 1.50 | 1.56 | 0.86 | 0.77 | 345.12 | 371.71 | 42.93 | 42.30 | 371.55 | 419.28 | 160.40 | 162.99 |
| 7 | 1.49 | 1.62 | 0.88 | 0.69 | 340.89 | 551.37 | 43.00 | 42.59 | 362.72 | 465.97 | 160.16 | 174.64 |
| 8 | 1.51 | 1.72 | 0.82 | 0.65 | 349.33 | 230.61 | 42.63 | 46.92 | 391.07 | 481.47 | 160.93 | 178.13 |
| 9 | 1.52 | 1.62 | 0.83 | 0.73 | 352.45 | 290.82 | 42.71 | 44.98 | 389.12 | 430.93 | 160.97 | 169.22 |
| 10 | 1.53 | 1.40 | 0.83 | 0.93 | 358.68 | 435.56 | 42.85 | 40.25 | 385.06 | 343.06 | 161.21 | 152.59 |
| 11 | 1.53 | 1.27 | 0.83 | 1.06 | 361.54 | 525.38 | 42.96 | 37.31 | 383.15 | 302.62 | 161.38 | 144.81 |
| 12 | 1.40 | 1.76 | 0.71 | 1.06 | 342.99 | 378.62 | 42.77 | 42.69 | 394.98 | 373.46 | 162.01 | 159.58 |
| 13 | 1.40 | 1.75 | 0.71 | 1.06 | 345.17 | 374.46 | 42.85 | 42.58 | 393.60 | 375.87 | 161.96 | 159.57 |
| 14 | 1.41 | 1.75 | 0.71 | 1.06 | 345.99 | 372.92 | 42.88 | 42.55 | 393.08 | 376.78 | 161.94 | 159.58 |
| 15 | 1.41 | 1.74 | 0.71 | 1.06 | 346.63 | 371.49 | 42.90 | 42.51 | 392.54 | 377.63 | 161.91 | 159.58 |

a) Here, bottom ash means the particles drained out of the furnace bottom.

## 4.2 Effect of the Lateral Profile of the Coal Feeding Rate

As shown in Fig. 4b, when the coal feeding rate in the middle cell is higher (case 4), inside the dense bed, the solid concentration in that cell is slightly lower than that in its neighboring cells, while the situation is the opposite inside the dilute zone. This can be attributed to the decrease in the average particle size of the bottom ash and circulating ash, as demonstrated in Tab. 2. At a fixed air flow rate, more particles will be entrained to the dilute zone when particles become smaller, and the fly ash and circulating ash mass flow rate will be higher as well. Besides, as presented in Fig. 5, with the further increase in the coal feeding rate in the middle cell (case 2 to case 4), the solid concentration deviation between the lateral cells increases, indicating that the lateral distribution of solid particles turns more uneven.

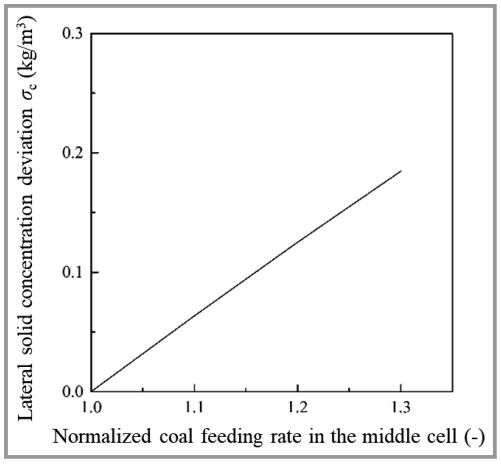


**Figure 5.** Variation of the lateral solid concentration deviation with the coal feeding rate in the middle cell.

## 4.3 Effect of the Lateral Profile of the Primary Air Flow Rate

Similar to the situation of varying the coal feeding rate, when the primary air flow rate in the middle cell turns higher (case 7), since more particles are entrained into the dilute zone, the solid concentration in the that cell is lower in the dense bed and higher in the dilute zone. However, as demonstrated in Fig. 4c, the reduction in the solid concentration in the dense bed becomes more obvious. Besides, at a fixed coal feeding rate, with more primary air in the middle cell, the fly ash and circulating ash mass flow rate will increase, leading to the decrease of the drainage rate of the bottom ash, which results in the increase of the average particle size of the bottom ash and circulating ash. Furthermore, with the further increase in the primary air flow rate

  

in the middle cell (case 5 to case 7), the solid concentration deviation between the lateral cells increases as well, but at a much higher rate compared to the situation of varying the coal feeding rate, as shown in Fig. 6. In other words, the lateral profile of the primary air flow rate has a much greater influence on the flow field inhomogeneity in the width direction compared to that of the coal feeding rate. On the other hand, considering that the uniform air distributing is difficult to achieve in industrial CFB boilers, the uneven air distributing may be the main cause of the lateral non-uniform distribution in the furnace.

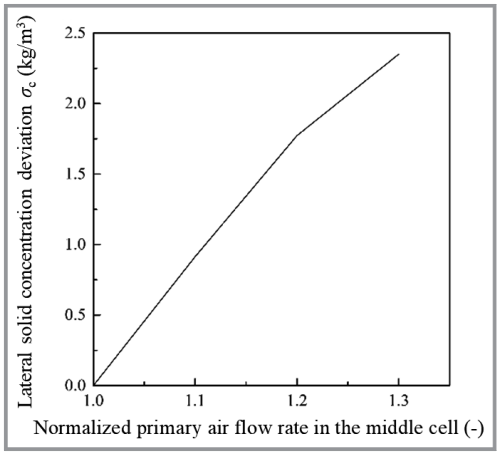


**Figure 6.** Variation of the lateral solid concentration deviation with the primary air flow rate in the middle cell.

### 4.4 Effect of the Lateral Profile of the Cyclone Efficiency

As demonstrated in Fig. 4d, the increase in the separation efficiency of the middle cyclone (case 11) will bring about the decrease in the solid concentration inside the dense bed and the increase of the same parameter inside the dilute zone as well but through a different mechanism. At a fixed coal feeding and primary air flow rate, the mass flow rate and average particle size of the fly ash will decrease with the increase of the cyclone efficiency, leading to the increase of the drainage rate of the bottom ash, which causes the circulating ash to become smaller. Since smaller particles are easier to be entrained, the solid concentration in the dilute zone and the circulating ash mass flow rate both increases. Moreover, as presented in Fig. 7, the positive or negative variation of the separation efficiency of the middle cyclone will both bring about the non-uniform lateral profile of the solid concentration (case 8–11), and it seems that decreasing the separation efficiency has a more pronounced effect.

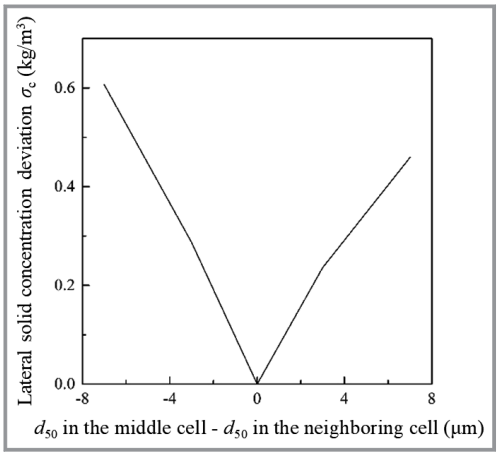


**Figure 7.** Variation of the lateral solid concentration deviation with the cyclone efficiency in the middle cell.

### 4.5 Effect of the Value of the Dispersion Coefficient

Fig. 8 and Tab. 2 demonstrate the variation of the lateral solid concentration deviation and the mass flow rate as well as the average particle size of the ash particles with the lateral dispersion coefficient. It can be concluded that with the increase of the lateral dispersion coefficient, the difference between the flow parameters in the middle cell and its neighboring cells decrease, meaning that stronger lateral dispersion will reduce the degree of the flow field inhomogeneity in the width direction.

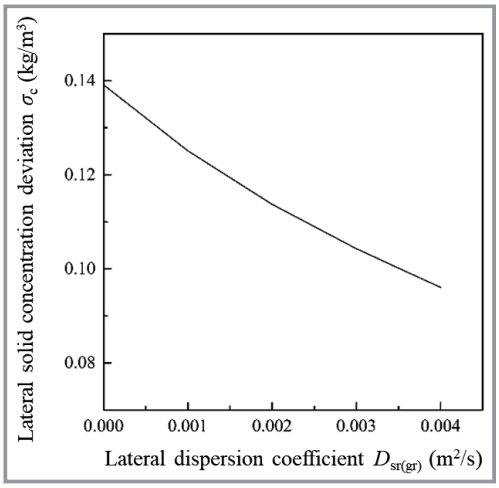


**Figure 8.** Variation of the lateral solid concentration deviation with the lateral dispersion coefficient.

## 5 Conclusions

The non-uniform lateral distribution in a 300-MW subcritical CFB boiler was investigated with a two-dimensional mass balance model capable of predicting the vertical and

  

lateral profile of the solid concentration as well as the ash mass flow rate and particle size. By specifying different non-uniform boundary conditions, the effect of four influential factors, namely the lateral profile of the coal feeding rate, primary air flow rate and cyclone efficiency as well as the value of the lateral dispersion coefficient, on the lateral non-uniform distribution was elucidated.

The results showed that the non-uniform lateral profile of these parameters affected the flow field inhomogeneity in the width direction, but through different mechanisms, and stronger lateral dispersion would reduce the degree of the flow field inhomogeneity. Besides, within the range of the operating conditions studied in this work, the uneven primary air distributing had a greater influence on the lateral non-uniform distribution in large-scale CFB boilers compared to the uneven coal feeding.

This work was financially supported by the National Key Research Plan (2019YFE0102100) and the C9 University Science and Technology Project (201903D421009).

## Symbols used

| | | |
|---|---|---|
| $A_{sec}$ | [$m^2$] | Section area between lateral cells |
| $C$ | [$kg\,m^{-3}$] | Solid concentration |
| $d_{50}/d_{99}$ | [µm] | Particle cut size/critical size for cyclone |
| $D_{gr}$ | [$m^2s^{-1}$] | Dispersion coefficient in the dense bed |
| $D_{sr}$ | [$m^2s^{-1}$] | Dispersion coefficient in the dilute zone |
| $H$ | [m] | Height of the CFB furnace |
| $h_i$ | [m] | Height of cell ($i$, $j = 1 - M$) |
| $M$ | [–] | Number of cells in the vertical direction |
| $\dot{m}_{l-1\rightarrow l}$ | [$kg\,s^{-1}$] | Solid mass rate from age group $l-1$ to $l$ |
| $\dot{m}_{l\rightarrow l+1}$ | [$kg\,s^{-1}$] | Solid mass rate from age group $l$ to $l+1$ |
| $\dot{m}_{shift,k,l}$ | [$kg\,s^{-1}$] | Solid mass rate caused by particle attrition |
| $N$ | [–] | Number of cells in the lateral direction |
| $N_k$ | [–] | Number of particle size groups |
| $N_l$ | [–] | Number of particle age groups |
| $Q_{pr}$ | [$Nm^3s^{-1}$] | Primary air flow rate |
| $W$ | [$kg\,s^{-1}$] | Solid mass rate |
| $x$ | [m] | Lateral distance |

## Greek letters

| | | |
|---|---|---|
| $\sigma_C$ | [$kg\,m^{-3}$] | Height-averaged solid concentration deviation |
| $\sigma_C(i)$ | [$kg\,m^{-3}$] | Solid concentration deviation at the height of cell ($i$, $j = 1 - M$) |

## Sub- and Superscripts

| | |
|---|---|
| *da* | Drainage of bottom ash |
| *down* | Downwards solid |
| *fa* | Feeding ash |
| *i* | Cell number in the vertical direction |
| *j* | Cell number in the lateral direction |
| *k* | Particle size group number |
| *l* | Particle age group number |
| *left* | Leftwards solid |
| *ra* | Recirculating ash |
| *right* | Rightwards solid |
| *up* | Upwards solid |

## References

[1] D. Rensner, J. Werther, *Part. Part. Syst. Charact.* **1993**, *10 (2)*, 48–55. DOI: https://doi.org/10.1002/ppsc.19930100204
[2] M. Kruse, J. Werther, *Chem. Eng. Process.* **1995**, *34 (3)*, 185–203. DOI: https://doi.org/10.1016/0255-2701(94)04004-4
[3] J. Werther, B. Hage, C. Rudnick, *Chem. Eng. Process.* **1996**, *35 (5)*, 381–391. DOI: https://doi.org/10.1016/0255-2701(96)80018-3
[4] B. Hage et al., *J. Chem. Eng. Jpn.* **1996**, *29 (4)*, 594–602. DOI: https://doi.org/10.1252/jcej.29.594
[5] O. Fiedler et al., *Powder Technol.* **1997**, *94 (1)*, 51–57. DOI: https://doi.org/10.1016/S0032-5910(97)03287-7
[6] B. Hage, J. Werther, *Powder Technol.* **1997**, *93 (3)*, 235–245. DOI: https://doi.org/10.1016/S0032-5910(97)03276-2
[7] J. Werther, *Powder Technol.* **1999**, *102 (1)*, 15–36. DOI: https://doi.org/10.1016/S0032-5910(98)00202-2
[8] V. Wiesendorf, J. Werther, *Powder Technol.* **2000**, *110 (1)*, 143–157. DOI: https://doi.org/10.1016/S0032-5910(99)00276-4
[9] J. Werther, T. Ogada, C. Philippek, *J. Inst. Energy* **1995**, *68 (475)*, 93–101.
[10] T. Ogada, J. Werther, *Fuel* **1996**, *75 (5)*, 617–626. DOI: https://doi.org/10.1016/0016-2361(95)00280-4
[11] C. Philippek, J. Werther, *J. Inst. Energy* **1997**, *70 (485)*, 141–150.
[12] J. Werther, T. Ogada, *Prog. Energy Combust. Sci.* **1999**, *25 (1)*, 55–116. DOI: https://doi.org/10.1016/S0360-1285(98)00020-3
[13] J. Werther, M. Saenger, *J. Chem. Eng. Jpn.* **2000**, *33 (1)*, 1–11. DOI: https://doi.org/10.1252/jcej.33.1
[14] M. Sänger, J. Werther, T. Ogada, *Fuel* **2001**, *80 (2)*, 167–177. DOI: https://doi.org/10.1016/S0016-2361(00)00093-4
[15] O. Malerius, J. Werther, *Chem. Eng. J.* **2003**, *96 (1)*, 197–205. DOI: https://doi.org/10.1016/j.cej.2003.08.018
[16] B. Leckner et al., *Fuel* **2003**, *83 (4)*, 477–486. DOI: https://doi.org/10.1016/j.fuel.2003.08.006
[17] I. Petersen, J. Werther, *Chem. Eng. Process.* **2004**, *44 (7)*, 717–736. DOI: https://doi.org/10.1016/j.cep.2004.09.001
[18] J. Werther, W. Xi, *Powder Technol.* **1993**, *76 (1)*, 39–46. DOI: https://doi.org/10.1016/0032-5910(93)80039-D
[19] M. Ghadiri et al., *Powder Technol.* **1994**, *80 (2)*, 175–178. DOI: https://doi.org/10.1016/0032-5910(94)80014-6
[20] J. Werther, J. Reppenhagen, *AIChE J.* **1999**, *45 (9)*, 2001–2010. DOI: https://doi.org/10.1002/aic.690450916
[21] J. Reppenhagen, J. Werther, *Powder Technol.* **2000**, *113 (1)*, 55–69. DOI: https://doi.org/10.1016/S0032-5910(99)00290-9

  

[22] C. Klett, E. U. Hartge, J. Werther, *Proc. Combust. Inst.* **2004**, *30 (2)*, 2947–2954. DOI: https://doi.org/10.1016/j.proci.2004.08.164
[23] E. U. Hartge, C. Klett, J. Werther, *Chem. Eng. Sci.* **2006**, *62 (1)*, 281–293. DOI: https://doi.org/10.1016/j.ces.2006.08.067
[24] C. Klett, E. U. Hartge, J. Werther, *AIChE J.* **2007**, *53 (4)*, 769–779. DOI: https://doi.org/10.1002/aic.11130
[25] K. Redemann, E. U. Hartge, J. Werther, *Powder Technol.* **2008**, *191 (1)*, 78–90. DOI: https://doi.org/10.1016/j.powtec.2008.09.009
[26] A. Thon, J. Werther, *Appl. Catal., A.* **2009**, *376 (1)*, 56–65. DOI: https://doi.org/10.1016/j.apcata.2009.11.036
[27] A. Thon et al., *Powder Technol.* **2011**, *214 (1)*, 21–30. DOI: https://doi.org/10.1016/j.powtec.2011.07.017
[28] J. Werther, *Powder Technol.* **1976**, *15 (2)*, 155–167. DOI: https://doi.org/10.1016/0032-5910(76)80044-7
[29] D. Bellgardt, J. Werther, *Powder Technol.* **1986**, *48 (2)*, 173–180. DOI: https://doi.org/10.1016/0032-5910(86)80076-6
[30] D. Bellgardt, M. Schoessler, J. Werther, *Powder Technol.* **1987**, *53 (3)*, 205–216. DOI: https://doi.org/10.1016/0032-5910(87)80095-5
[31] J. Werther, E. U. Hartge, M. Kruse, *Powder Technol.* **1992**, *70 (3)*, 293–301. DOI: https://doi.org/10.1016/0032-5910(92)80065-5
[32] J. Vollert, J. Werther, *Chem. Eng. Technol.* **1994**, *17 (3)*, 201–209. DOI: https://doi.org/10.1002/ceat.270170309
[33] R. Koenigsdorff, J. Werther, *Powder Technol.* **1995**, *82 (3)*, 317–329. DOI: https://doi.org/10.1016/0032-5910(94)02935-H
[34] M. Kruse, H. Schoenfelder, J. Werther, *Can. J. Chem. Eng.* **1995**, *73 (5)*, 620–634. DOI: https://doi.org/10.1002/cjce.5450730505
[35] B. Hirschberg, J. Werther, *AIChE J.* **1998**, *44 (1)*, 25–34. DOI: https://doi.org/10.1002/aic.690440105
[36] E. U. Hartge, K. Luecke, J. Werther, *Chem. Eng. Sci.* **1999**, *54 (22)*, 5393–5407. DOI: https://doi.org/10.1016/S0009-2509(99)00273-0
[37] P. Schlichthaerle, J. Werther, *Powder Technol.* **2001**, *120 (1)*, 21–33. DOI: https://doi.org/10.1016/S0032-5910(01)00342-4
[38] J. Werther, *Chem. Eng. Sci.* **1980**, *35 (1–2)*, 372–379. DOI: https://doi.org/10.1016/0009-2509(80)80109-6
[39] J. Werther, *Chem. Eng. Sci.* **1992**, *47 (9–11)*, 2457–2462. DOI: https://doi.org/10.1016/0009-2509(92)87076-3
[40] H. Schoenfelder, M. Kruse, J. Werther, *AIChE J.* **1996**, *42 (7)*, 1875–1888. DOI: https://doi.org/10.1002/aic.690420709
[41] T. Knoebig, K. Luecke, J. Werther, *Chem. Eng. Sci.* **1999**, *54 (13)*, 2151–2160. DOI: https://doi.org/10.1016/S0009-2509(98)00359-5
[42] K. Luecke, E. U. Hartge, J. Werther, *Int. J. Chem. React. Eng.* **2004**, *2 (1)*, A11. DOI: https://doi.org/10.2202/1542-6580.1135
[43] J. Werther, E. U. Hartge, *Ind. Eng. Chem. Res.* **2004**, *43 (18)*, 5593–5604. DOI: https://doi.org/10.1021/ie030760t
[44] R. Wischnewski et al., *Particuology.* **2009**, *8 (1)*, 67–77. DOI: https://doi.org/10.1016/j.partic.2009.08.001
[45] C. Reimers, J. Werther, G. Gruhn, *Chem. Eng. Process.* **2007**, *47 (1)*, 138–158. DOI: https://doi.org/10.1016/j.cep.2007.07.015
[46] C. Reimers, J. Werther, G. Gruhn, *Powder Technol.* **2008**, *191 (3)*, 260–271. DOI: https://doi.org/10.1016/j.powtec.2008.10.012
[47] D. Schwier et al., *Chem. Prod. Process Model.* **2009**, *4 (1)*, 24. DOI: https://doi.org/10.2202/1934-2659.1227
[48] M. Dosta, S. Heinrich, J. Werther, *Powder Technol.* **2010**, *204 (1)*, 71–82. DOI: https://doi.org/10.1016/j.powtec.2010.07.018
[49] I. Alaathar et al., *Powder Technol.* **2013**, *238*, 132–141. DOI: https://doi.org/10.1016/j.powtec.2012.03.048
[50] J. Haus, E. U. Hartge, S. Heinrich, et al., *Powder Technol.* **2016**, *316*, 628–640. DOI: https://doi.org/10.1016/j.powtec.2016.12.022
[51] J. Haus et al., *Int. J. Greenhouse Gas Control.* **2018**, *72*, 26–37. DOI: https://doi.org/10.1016/j.ijggc.2018.03.004
[52] M. Kramp et al., *Chem. Eng. Technol.* **2012**, *35 (3)*, 497–507. DOI: https://doi.org/10.1002/ceat.201100438
[53] A. Thon et al., *Appl. Energy* **2014**, *118*, 309–317. DOI: https://doi.org/10.1016/j.apenergy.2013.11.023
[54] J. Haus et al., *Energy Technol.* **2016**, *4 (10)*, 1263–1273. DOI: https://doi.org/10.1002/ente.201600102
[55] T. Song et al., *Int. J. Greenhouse Gas Control.* **2018**, *70*, 22–31. DOI: https://doi.org/10.1016/j.ijggc.2018.01.005
[56] S. Y. Yin et al., *Energy Fuels* **2018**, *32 (11)*, 11674–11682. DOI: https://doi.org/10.1021/acs.energyfuels.8b02849
[57] J. Haus et al., *Fuel* **2019**, *236*, 166–178. DOI: https://doi.org/10.1016/j.fuel.2018.08.151
[58] S. Wang et al., *Fuel* **2020**, *270 (C)*, 117464. DOI: https://doi.org/10.1016/j.fuel.2020.117464
[59] J. Werther, *Chem. Ing. Tech.* **1977**, *49 (10)*, 777–785. DOI: https://doi.org/10.1002/cite.330491003
[60] J. F. Lu et al., *Heat Transfer-Asian Res.* **2002**, *31*, 540–550. DOI: https://doi.org/10.1002/htj.10056
[61] H. R. Yang et al., *Energy Fuels* **2009**, *23*, 2886–2890. DOI: https://doi.org/10.1021/ef900025h
[62] A. Gómez-Barea, B. Leckner, *Prog. Energy Combust. Sci.* **2010**, *36*, 444–509. DOI: https://doi.org/10.1016/j.pecs.2009.12.002
[63] H. R. Yang et al., *Chem. Eng. Sci.* **2005**, *60*, 5603–5611. DOI: https://doi.org/10.1016/j.ces.2005.04.081
[64] X. W. Ke, *Comprehensive modeling study on NOx emission characteristics of circulating fluidized bed combustion*, Ph.D. Thesis, Tsinghua University **2021**.
[65] N. Hu, *Study on Heterogeneity in Combustion System of Circulating Fluidized Bed Boiler*, Ph.D. Thesis, Tsinghua University **2013**.
[66] N. Hu et al., *J. Chin. Soc. Power Eng.* **2016**, *3*, 168–171.
[67] D. Y. Liu et al., *J. Eng. Thermophys.* **2009**, *30*, 529–532. DOI: https://doi.org/10.3321/j.issn:0253-231X.2009.03.044
[68] J. Olsson, D. Pallares, F. Johnsson, *Chem. Eng. Sci.* **2012**, *74*, 148–159. DOI: https://doi.org/10.1016/j.ces.2012.02.027
[69] P. Schlichthaerle, J. Werther, *Powder Technol.* **2001**, *120*, 21–33. DOI: https://doi.org/10.1016/s0032-5910(01)00342-4
[70] H. R. Yang et al., *J. Eng. Therm. Power* **2001**, *16*, 395–398.
[71] L. Gan et al., *Powder Technol.* **2013**, *243*, 1–8. DOI: https://doi.org/10.1016/j.powtec.2013.03.021
[72] O. Oke, B. V. Wachem, L. Mazzei, *Chem. Eng. Res. Des.* **2016**, *114*, 148–161. DOI: https://doi.org/10.1016/j.cherd.2016.08.014


  